Langmuir
Article
pubs.acs.org/Langmuir

A One-Step Continuous Synthesis of Carbon-Supported Pt Catalysts Using a Flame for the Preparation of the Fuel Electrode

In Dae Choi,[†] Hyunmin Lee,[†] Yoon-Bo Shim,[‡] and Donggeun Lee*[,†]

[†]*School of Mechanical Engineering, Pusan Clean Coal Center, RIMT, Pusan National University, San 30, Jangjeon dong, Geumjeong gu, Busan 609-735, South Korea, and* [‡]*Department of Chemistry, Pusan National University, San 30, Jangjeon dong, Geumjeong gu, Busan 609-735, South Korea*

Received February 4, 2010. Revised Manuscript Received March 6, 2010

We introduce a novel single-step method capable of a continuous production of Pt catalysts supported on carbon agglomerates for the preparation of the fuel electrode. An acetylene−air diffusion flame is employed as heat and carbon sources, and $Pt(acac)_2$-containing xylene droplets are injected into the flame. A sampling height from the burner top, initial concentration of $Pt(acac)_2$, and acetylene flow rate are demonstrated as efficient systematic parameters to control the size (from 2 to 7 nm) and surface coverage (or content up to 60 wt %) of spherical Pt particles. A variety of characterization methods manifest that the Pt exists mostly in a metallic form and carbon agglomerates are in good crystalline order. Finally, the electrochemical activity is confirmed to be higher than 74.9 $m^2\ g^{-1}$ Pt, more efficient than an equivalent commercial (E-TEK 10 wt % Pt) catalyst.

1. Introduction

A proton exchange membrane fuel cell (PEMFC) has attracted increasing attention in power-related scientific and industrial fields because of its high conversion efficiency from hydrogen to electricity that is not limited by Carnot cycle of thermal process.[1] One of the biggest challenges, however, is how to reduce the high cost of the system, mainly due to use of precious metal catalyst of platinum (Pt). This can be surmounted either by reducing the amount of Pt or by replacing Pt with a less expensive metal like ruthenium.[2] An efficient way to minimize the amount of Pt is to use smaller Pt particles with narrower size distribution and better dispersion on a carbon-based support.

For this purpose, many researchers have proposed various efficient methods such as impregnation,[2] electrodeposition of colloidal Pt particles,[3] chemical reduction[4,5] along with ultrasonic treatment,[6] multistep pyrolysis with supercritical CO_2 gas,[7] and polymer homogenization.[8] Many of the aforementioned methods enabled to reduce the diameters of Pt particles to 2−5 nm[2,4,6−8] at which Pt catalysts are most electrochemically active;[9] however, surface dispersion of Pt on carbon supports seemed to be not so good.[4−6] Chen and Xing[8] achieved an excellent dispersion of Pt on carbon supports by using an organic polymer to minimize Pt aggregation. More recently, Shimizu et al.[10] reported a wet-chemistry method capable of fast reduction of Pt salt to the surface of preexisting carbon nanotubes in methanol with a high efficiency. But, the result manifested the particles were possibly coated with amorphous carbon, resulting from incomplete formation of carbon nanotubes. Despite those benefits, all methods are essentially a multistep process which requires further time-consuming steps such as filtration, purification, and drying. The production rate of the methods is thus lowered. Shanmugam and Simon[11] proposed a single-step method that is facile as well as solvent- and catalyst-free with easy handling. They used a direct heating of $Pt(acac)_2$ powder in a closed metal container and a subsequent slow cooling to room temperature. Thermal decomposition of the powder in the closed reactor, however, generated Pt embedded in carbon matrix rather than Pt on carbon supports, which is not appropriate for the purpose of fuel electrode.

A flame synthesis method might offer an alternative route to resolve the challenge because the method enables to continuously produce nanoparticles with a single step by virtue of the self-purifying process in flame.[12,13] The method offers another benefit of easy scale-up for large-scale production (700 g/h) of various nanoparticles such as silica[14] and titania.[15] However, particle aggregation is almost inevitable, though a few ways[13,16−18] have been proposed to control the aggregation. Carbon agglomerates are readily produced at high concentration directly from a gaseous fuel−air diffusion flame by adjusting the air−fuel ratio.[19,20] It is interesting to note that as the carbon agglomerates is tested for a support of Pt, the agglomeration of carbon particles in flame is not a problem; rather, it enables to enhance electrical

*Corresponding author: Tel +82-51-510-2365; Fax +82-51-512-5236; e-mail donglee@pusan.ac.kr.

(1) Li, X. *Principles of Fuel Cells*, 1st ed.; Taylor & Francis: New York, 2006.
(2) Godoi, D. R. M.; Perez, J.; Villullas, H. M. *J. Electrochem. Soc.* **2007**, *154*, B474–B479.
(3) Duarte, M. M. E.; Pilla, A. S.; Sieben, J. M.; Mayer, C. E. *Electrochem. Commun.* **2006**, *8*, 159–164.
(4) Liang, Y.; Zhang, H.; Yi, B.; Zhang, Z.; Tan, Z. *Carbon* **2005**, *43*, 3144–3152.
(5) Huang, J.-E.; Guo, D.-J.; Yao, Y.-G.; Li, H.-L. *J. Electroanal. Chem.* **2005**, *577*, 93–97.
(6) Tong, H.; Li, H. L.; Zhang, X. G. *Carbon* **2007**, *45*, 2424–2432.
(7) Smirnova, A.; Dong, X.; Hara, H.; Vasiliev, A.; Sammes, N. *Int. J. Hydrogen Energy* **2005**, *30*, 149.
(8) Chen, M.; Xing, Y. *Langmuir* **2005**, *21*, 9334–9338.
(9) Li, W.; Liang, C.; Zhou, W.; Qiu, J.; Li, H.; Sun, G.; Xin, Q. *Carbon* **2004**, *42*, 436–439.
(10) Shimizu, K.; Wang, J. S.; Cheng, I. F.; Wai, C. M. *Energy Fuels* **2009**, *23*, 1662–1667.
(11) Shanmugam, S.; Simon, U. *Chem.—Eur. J.* **2008**, *14*, 8776–8779.
(12) Pratsinis, S. E. *Prog. Energy Combust. Sci.* **1998**, *24*, 197–219.
(13) Lee, D.; Yang, S.; Choi, M. *Appl. Phys. Lett.* **2001**, *79*, 2459–2461.
(14) Kammler, H. K.; Mueller, R.; Senn, O.; Pratsinis, S. E. *AIChE J.* **2001**, *47*, 1533–1543.
(15) Kammler, H. K.; Pratsinis, S. E. *J. Mater. Res.* **2003**, *18*, 2670–2676.
(16) Lee, D.; Choi, M. *J. Aerosol Sci.* **2000**, *31*, 1145–1163.
(17) Lee, D.; Choi, M. *J. Aerosol Sci.* **2002**, *33*, 1–16.
(18) Vemury, S.; Pratsinis, S. E.; Kibbey, L. *J. Mater. Res.* **1997**, *12*, 1031–1042.
(19) Higgins, K.; Jung, H.; Kittelson, D. B.; Roberts, J. T.; Zachariah, M. R. *J. Phys. Chem. A* **2002**, *106*, 96–103.
(20) Ernst, F. O.; Buchel, R.; Strobel, R.; Pratsinis, S. E. *Chem. Mater.* **2008**, *20*, 2117–2123.

conductivity of carbon electrodes by providing interparticle bridges. Hence, a coinjection of any type of Pt precursor into the flame is highly expected to realize the one-step continuous production of Pt nanoparticles on carbon agglomerates.

Despite these great benefits and potentials, it is very surprising to hardly find relevant studies. To the best of our knowledge, Ernst et al.'s two-burner system[20] is the only one that can produce Pt particles (5−15 nm) on carbon supports continuously with a single step. They also found that the single-burner system, i.e., the coinjection of $Pt(acac)_2$−xylene solution into a CH_4-O_2 premixed flame, always generated carbon-embedded Pt particles (2−5 nm). Therefore, there is still a big challenge for reducing Pt size to 2−5 nm as well as narrowing the size distribution. To resolve the challenge is the objective of this study. An acetylene−air diffusion flame is employed as a carbon source as well as a heat source. The flame burner consisting of several concentric tubes enables to inject anther inert gas so as to isolate the carbon inception from Pt formation. A sampling height of catalyst particles from the burner top is varied to check the controllability of Pt size. Either a concentration of Pt precursor in an organic solvent or acetylene flow rate is altered so as to control the dispersion of Pt particles. As-received carbon-supported Pt (Pt/C) particles are characterized by high-resolution transmission electron microscopy, energy-dispersive spectroscopy, X-ray diffraction, X-ray photoelectron spectroscopy, and Raman scattering. Electrocatalytic properties of the Pt/C particles are examined by cyclic voltammetry and compared with an equivalent commercial catalyst.

2. Experimental Section

Platinum(II) acetylacetonate ($Pt(acac)_2$, Aldrich, 97%) powder was dissolved in xylene with a concentration of 0.25 wt %. The $Pt(acac)_2$−xylene solution was nebulized to 1−3 μm droplets in an ultrasonic atomizer by compressed air of 30 psi and then fed to a burner through a heated tube as seen in Figure 1. The burner consisting of five concentric stainless steel tubes was essentially similar to those used in our previous studies.[13,16,17] The carrier gas (air) containing the solution droplets flows through the center tube at 2.4 L min^{-1}. A shield gas of nitrogen flows at 2.0 L min^{-1} through the first annular space between the center and the next tube. Acetylene (C_2H_2) and dry air were injected through the second and third concentric annuli at 0.14 and 1.4 L min^{-1}, respectively, forming a coflow diffusion flame. In order to stabilize the flame, argon gas flows at 20 L min^{-1} through the outer tube containing a honeycomb with 100 openings cm^{-2} and two fine meshes.[13,16,17]

The injection speed of the shield gas was 10 times larger than that of the C_2H_2, so as to retard the decomposition of the $Pt(acac)_2$ precursor to after carbon inception. After a number of preliminary tests, the flow rates of gases were determined to result in a good dispersion of Pt particles on carbon supports and kept constant as the basic gas condition unless otherwise noted. Such Pt/C particles were thermophoretically deposited to a water-cooled quartz tube for further characterization of the samples. As depicted in Figure 1, vertical location of the quartz tube was adjusted precisely with a 1D traversing system, while the tube is reciprocating horizontally back and forth by a pneumatic cylinder so as to prevent any undesirable heating of the deposited particles.

By measuring the mass of deposits in an hour, the apparent production rate of this method is estimated to be on the order of 10 mg/h, far less than the value of Ernst et al.'s method (~3 g/h).[20] The difference in the production rate is mainly attributed to the difference in the feeding rate of xylene; in our case, xylene is sprayed via our atomizer at ~0.1 cm^3 min^{-1}, 20−50 times smaller than their value of 2.2−5 cm^3 min^{-1}. Another possible reason is that our deposition method is much less efficient than the conventional filter. It should be recalled here that the production rate

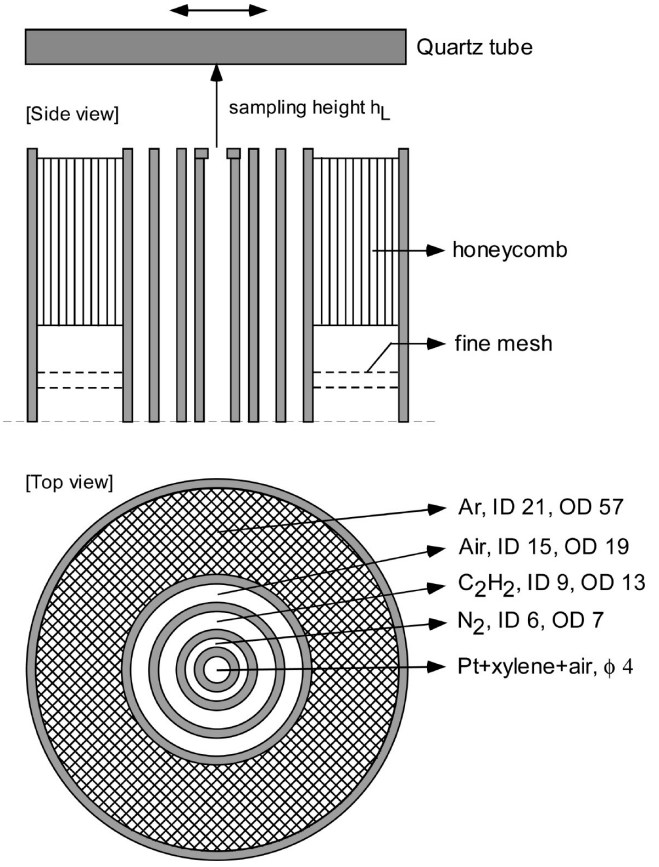

Figure 1. Schematic of the acetylene−air diffusion flame burner used for the generation of Pt/C nanoparticles (not to scale). Numbers for ID, OD, and ϕ are in millimeters.

can be greatly improved either by employing more efficient deposition tools such as Ahn et al.'s sampling probe[21] capable of minimizing particle loss without further particle growth or by a number of variations in burner design with fine-tuning of gas flow rates. Of greater interest is therefore the demonstration of the capability of the present *continuous* method in the aspect of whether the size and surface coverage of Pt are controllable or not in the size range of interest (2−5 nm).

As-deposited Pt/C particles were then dispersed in ethanol with an ultrasonicator. A few milliliters of Pt/C-ethanol suspension were dropped on a carbon-coated grid and then dried at room temperature. Size, morphology, and elemental composition of the Pt/C particles were characterized with a high-resolution transmission electron microprobe (HRTEM; JEOL 2100F, 200 kV) equipped with energy dispersive spectroscopy (EDS). Lattice spacing of Pt particles was measured from HRTEM images and compared with JCPDS database to ensure whether Pt exists as a metallic form or not. Crystalline phases of the dried powder samples were also verified by X-ray diffraction (XRD; D/Max-2400, Rigaku). The XRD measurement was performed by scanning the angle of 2θ in the range of 30°−85° with 4° min^{-1}, while irradiating Cu Kα X-ray (30 kV, 40 mA, 0.152 18 nm). Pt content of the dried Pt/C powder was estimated by measuring the mass loss of the sample when heating the Pt/C powder in air at 20 °C min^{-1} using thermogravimetric analyzer (TGA; Q50, TA Instruments). Surface chemical states of Pt and C particles were characterized by X-ray photoelectron spectroscopy (XRS; ESCALAB 250 XPS spectrometer) upon irradiating Al Kα X-ray with a resolution of 0.45 eV. Crystallinity of carbon spherules was further analyzed by Raman spectroscopy (inVia Raman microscope, Renishaw) using

(21) Ahn, K. H.; Jung, C. H.; Choi, M.; Lee, J. S. *J. Nanoparticle Res.* **2001**, *3*, 161–170.

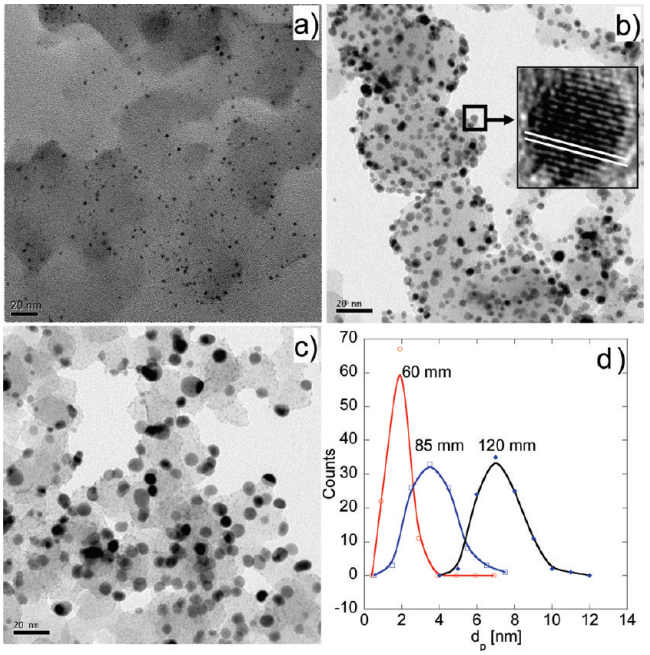

Figure 2. (a−c) TEM images of flame-made Pt/C particles captured at different heights (h_L) such as 60, 85, and 120 mm under the basic gas condition and (d) corresponding size distributions of Pt particles. The bar represents 20 nm. A hundred particles are counted for each profile in (d).

514.5 nm Ar laser light. Electrochemical activity of Pt/C samples was characterized by a cyclic voltammetry (CV) using a potentiostat/galvanostat (Kosentech model PT-2, South Korea),[22] upon scanning the range of −0.2 to 1.0 V at a rate of 100 mV s^{-1}. Glassy carbon (area = 19.6 mm^2) modified by the present catalysts in 0.5 M H_2SO_4 solution, an Ag/AgCl (in saturated KCl), and a Pt wire were used as working, saturated reference, and counter electrodes, respectively.

3. Results and Discussion

Figures 2a−c show an evolution of Pt spheres on carbon agglomerates along the flame. At the lowest sampling height h_L = 60 mm from the burner top, tiny Pt spheres as small as 1.9 ± 0.6 nm are observed. The Pt particles obviously grow to 3.5 ± 1.3 nm, 25 mm downstream of the flame, together with a great increase in their population, suggesting the coexistence of vigorous nucleation and coalescence of Pt particles in the region. Comparison of Figures 2b,c however reveals that Pt particles grow with decrease in the population, which indicates the coalescence-driven growth of Pt particles. Inset of Figure 2b shows that dark spheres are monocrystals whose lattice spacing (2.26 ± 0.01 Å) is very close to the value of metallic Pt (111). On the other hand, EDS spectra reveal that the composite particles in Figures 2a−c consist of carbon and Pt (see Figure S1), suggesting that the light gray chainlike supports are carbon agglomerates and the darker spots are likely metallic Pt.

Of particular interest is to note that Pt particle sizes are controllable simply by altering sampling heights as seen in Figure 2d. As a result, the geometric mean diameter of Pt particles increases from 1.8 nm to 4.1 and 6.2 nm, when increasing the h_L from 60 mm to 85 and 120 mm, respectively. At the same time, geometric standard deviation (GSD) of Pt particles gradually decreases from 1.40 to 1.32 and 1.19 along the flame, while standard deviation representing the width of size distribution on the linear scale (as seen in Figure 2d) varies from 0.57 to 1.13 and 1.16 nm, respectively. The GSD value of 1.40 at h_L = 60 mm, being pretty close to 1.46 for aerosol coagulation in free-molecular regime, is indicative of the gas-phase formation of Pt particles prior to their coagulation with the carbon agglomerates.[12,23] Once Pt spheres deposit to the carbon surface, their movement is likely constrained by the surface, in such a way to suppress the coagulation with other Pt neighbors. On the other hand, Figures 2a−c show that the size of carbon primary particles is hardly changed at $h_L \leq$ 85 mm; however, the size seems to decrease further downstream of the flame (at h_L = 120 mm) probably due to carbon combustion by the presence of Pt.[24] The size reduction of carbon primaries can force Pt spheres to get closer, enhancing the limited coagulation between Pt spheres to some degree. This might be a mechanism underlying the Pt growth in the region of 85 mm ≤ h_L ≤ 120 mm.

Table 1. Yields of Carbon and Pt of Pt/C Particles Shown in Figures 2a−c and 4a,b

	along flame at the basic condition			less $Pt(acac)_2$	less C_2H_2
	Figure 2a	Figure 2b	Figure 2c	Figure 4a	Figure 4b
carbon yield [%]	0.101	0.057	0.045	0.065	0.015
Pt yield [%]	3.2	22.7	20.1	33.0	23.7

According to Ernst et al.,[20] the carbon yield χ_c was estimated by $\chi_c = m_{dep}(1 - C_{Pt})/m_c$ where m_{dep} was the mass deposition rate of particles on the quartz tube, C_{pt} was Pt content of the product powder that can be determined by TGA, and m_c was the total mass of carbon available in $Pt(acac)_2$−xylene solution that was a sole carbon source. In our diffusion flame, however, flame-generated carbon particles dominate the entire carbon agglomerates. Thus, the m_c is replaced by the total mass flow rate of carbon in the fuel of C_2H_2. Similarly, the Pt yield χ_{Pt} is estimated by $\chi_{Pt} = m_{dep}C_{Pt}/m_{Pt}$ where the mass feeding rate of Pt m_{pt} is estimated from the feeding rate of xylene and concentration of $Pt(acac)_2$ in it. Table 1 summarizes the yields of carbon and Pt of Pt/C particles shown in Figures 2a−c and 4a,b.

In Table 1, carbon yield is very low, only on the order of 0.05%, which is attributed to significant consumption of fuel-born carbon during the combustion of C_2H_2. The gradually decreasing carbon yield along the flame indicates carbon inception does likely end at $h_L \leq$ 60 mm, and the carbon is getting consumed via catalytic combustion. At the same time, the Pt yield greatly increases at 60 mm ≤ h_L ≤ 85 mm, which is consistent with the TEM observation between Figures 2a,b. Also, this suggests that the carbon inception occurs prior to the Pt formation by virtue of N_2 injection and high injection speed of the precursor droplets, in accordance with our main idea. At 85 mm ≤ h_L ≤ 120 mm, the almost invariant Pt yield implies no Pt source is available for further growth. Thus, the Pt growth seen in between Figures 2b,c is mainly attributed to the limited coalescence between particles on consuming carbon agglomerates.

Crystallinity of the Pt/C samples captured at h_L = 85 and 120 mm is examined by the XRD. Figure 3a shows that XRD patterns of the two samples consist of four major peaks of metallic Pt at 39.7°, 46.2°, 67.1°, and 81° in 2θ unit and a small peak at 41.4° as a signature of a sample holder. The biggest peak of Pt is deconvoluted. The peak width of Pt (111) is used to estimate the crystallite size of Pt by using Scherrer equation. As a result, the crystallite sizes of samples at h_L = 85 and 120 mm are ca. 4.5 and 7.5 nm,

(22) Rahman, A.; Noh, H.-B.; Shim, Y. B. *Anal. Chem.* **2008**, *80*, 8020–8027.

(23) Friedlander, S. K. *Smokes, Dust and Haze*; John Wiley & Sons: New York, 1977; pp 195−253.

(24) Stein, H. J. *Appl. Catal., B* **1996**, *10*, 69–82.

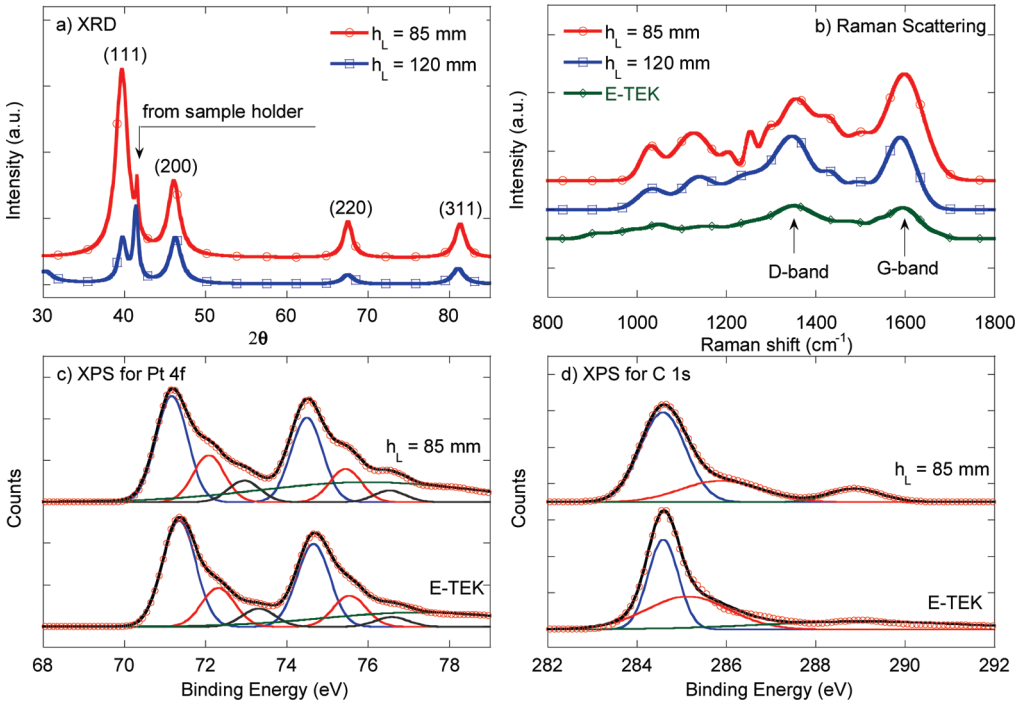

Figure 3. Characterization of the present samples in comparison with E-TEK commercial Pt/C sample: (a) XRD patterns, (b) Raman shifts for the samples seen in Figures 2b,c. XPS spectra for (c) Pt 4f and (d) C 1s core level of the sample in Figure 2b.

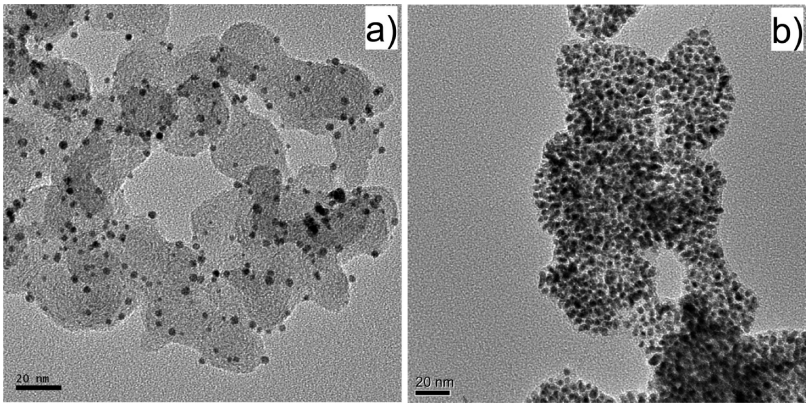

Figure 4. TEM image of Pt/C particles obtained (a) by lowering the content of $Pt(acac)_2$ in xylene or (b) by lowering flow rate of C_2H_2, from the basic condition corresponding to Figure 2b.

respectively, which are reasonably consistent with the results from TEM analysis (see Figure 2d). Raman scattering is also used to evaluate atomic disorder of the carbon particles that might be a measure of relative ohmic resistance of carbon-based electrode. In Figure 3b, the D and G bands at 1355 and 1596 cm^{-1} represent the sp^3- and sp^2-hybridized carbons, indicating disordered and ordered carbon graphene structures, respectively.[6] It is interesting to note that the intensity ratio of the D band to the G band (I_D/I_G) increases from 0.76 to 1.03 with increase of h_L from 85 and 120 mm, suggesting that carbon supports are more crystallized at lower flame height. This seems to be unreasonable because such a graphitization gets often profound downstream of a flame due to longer sample heating. A possible reason is that the presence of Pt might destruct the crystalline structure of carbon in flame due to its catalytic effect of carbon oxidation. It is here noted that the values of I_D/I_G of the flame samples are both lower than that of a commercial E-TEK catalyst (1.08), suggesting that the present electrode materials are better crystallized. Hence, the Pt/C catalyst at h_L = 85 mm is chosen for the PEMFC catalytic anode and will be compared with the commercial E-TEK catalyst in the aspect of electrochemical activity.

The oxidative states of the Pt/C catalysts are examined by the XPS. Figure 3c shows that the Pt 4f core-level XPS spectra of the Pt/C catalyst are mainly composed of three pairs of doublets. The highest doublet (at 71.2 and 74.5 eV) is the signal of metallic Pt.[25] The second highest doublet (at 72.1 and 75.4 eV), 1 eV blue-shifted from the peaks of Pt, is assigned to Pt[II] states as in PtO or $Pt(OH)_2$. The weakest third doublet at 72.9 and 76.5 eV suggests the minor level of Pt[IV] as in PtO_2 exists in the present catalysts. A similar trend is observed in E-TEK catalyst; however, the total oxidative states of the E-TEK catalyst seem to be slightly lower than those of the flame sample. The higher oxidative states in our sample are probably due to the high-temperature heating of Pt/C particles in flame where oxygen is rich. Figure 3d shows the C 1s core-level XPS spectra mainly consist of three peaks at 284.6, 285.5, and 288.9 eV, corresponding to C−C, C−O, and C═O

(25) Wu, G.; Chen, Y.-S.; Xu, B.-Q. *Electrochem. Commun.* **2005**, *7*, 1237–1243.

groups.[26] The higher level of C═O in the present Pt/C catalyst is likely correlated with the aforementioned higher oxidative states of Pt. According to the bifunctional mechanism of methanol electrooxidation,[25,27] the higher level of oxidative states of Pt in our catalyst can enhance the electrocatalytic activity for direct methanol fuel cell.

As mentioned in the Introduction, the controllability of Pt surface coverage on carbon supports becomes another key factor to evaluate the present method in the aspect of efficient usage of Pt. In order to decrease the surface coverage, the initial content of $Pt(acac)_2$ in xylene was set to decrease by a factor of 4 (to 0.06 wt %), as compared to the basic condition used for Figure 2b. As expected, Figure 4a shows a discernible decrease in surface coverage of Pt spheres. Since another control parameter would be the flow rate of C_2H_2 that is a carbon source, decreasing carbon yield can increase the Pt content relatively. In this regard, the C_2H_2 flow rate is decreased to 0.12 L min^{-1} with respect to the basic condition. Figure 4b denotes that this trial is quite successful so that the Pt surface coverage becomes greatly enhanced with no remarkable change of Pt size. Table 1 shows when reducing $Pt(acac)_2$ concentration of the xylene solution (Figure 4a), the carbon yield increases from the basic condition corresponding to Figure 2b, as expected. When the flow rate of C_2H_2 decreases (Figure 4b), Table 1 also shows that the carbon yield is dramatically decreased from in the basic condition while the Pt yield is almost the same. This supports the inference that the fuel C_2H_2 works as a carbon source as well as a heat source. In addition, the fairly low level of Pt yield indicates the present deposition method is not so efficient.

Pt contents of the particles shown in Figures 2b, 4a, and 4b are estimated to 25, 10, and 60 wt % by TGA, respectively (see Figure S2). It is also found that the samples in Figures 2b,c have similar levels of Pt, and the sample in Figure 2a contains only 2.5 wt % of Pt. Since the level of 60 or 2.5 wt % seems to be too high or too low for the use of catalytic electrode, the two samples of 10 and 25 wt % are further examined in the electrochemical characteristics.

Figure 5 shows cyclic voltammograms (CV) recorded for the present two catalysts and the commercial E-TEK catalyst of 10 wt % Pt, in which the potential was expressed with respect to that of the saturated reference electrode (SRE; Ag/AgCl). The electrochemical behaviors of the three catalysts are all similar; hydrogen adsorption/desorption peaks are observed in the potential region of −0.2 to 0.1 V, and the reduction peak of the Pt oxide clearly appears at the potential of ~0.4 V. This is quite consistent with the previous observations for Pt/C catalysts.[2,5,6,8] The electrochemically active surface area[8] of Pt particles S_{act}, in units of $m^2\ g^{-1}$ Pt, is estimated from the CV curves for each of the samples by $S_{act} = Q/vq_H^0$, where Q, in units of mA V g^{-1} Pt, is the integrated area of the hydrogen adsorption region per unit mass of Pt, v is the scan rate (mV s^{-1}), and q_H^0 is the charge for monolayer hydrogen adsorption on Pt that is equal to 0.21 mC cm^{-2}. As a result, the S_{act} for the 10 wt % Pt/C catalyst is ca. 74.9 $m^2\ g^{-1}$ Pt, slightly larger than that of the equivalent E-TEK catalyst (64.7 $m^2\ g^{-1}$ Pt). The maximum value of S_{act} is 82.5 $m^2\ g^{-1}$ Pt for the 25 wt % Pt/C catalyst. We would like to emphasize here that the present flame method seems to realize the concept of single-step continuous production of Pt/C catalysts with the competitive electrochemical activity, more interestingly under controls of size and dispersion of Pt on carbon agglomerates.

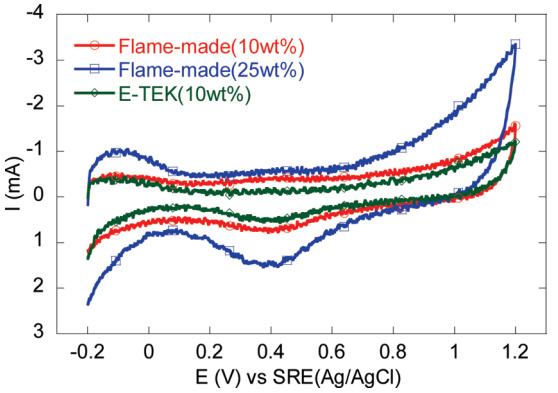

Figure 5. Comparison of cyclic voltammograms between the present samples with different Pt wt % and commercial sample.

4. Conclusion

In this article, we introduced a novel single-step method capable of a continuous production of Pt catalysts supported on carbon agglomerates. Acetylene−air diffusion flame was used as heat and carbon sources, to which $Pt(acac)_2$-containing xylene droplets are injected. Simply varying the sampling heights, we confirmed that the size of metallic Pt spheres is well controlled from 2 to 7 nm. In addition, we demonstrated that either the flow rate of acetylene or the initial content of $Pt(acac)_2$ in xylene is an effective parameter to control the surface dispersion of Pt spheres. A variety of characterization methods manifested that the Pt existed mostly in a metallic form and carbon agglomerates were in good crystalline order. Finally, we confirmed that the electrochemical activity is better as compared to the commercial catalyst.

Acknowledgment. This work was supported by the National Research Foundation of Korea (NRF) Grant funded by the Korea government (MEST) (No. 2009-0086170).

Supporting Information Available: Typical EDS spectrum of flame-made Pt/C catalytic particles, and TGA profiles of the present Pt/C catalysts with different Pt contents. This material is available free of charge via the Internet at http://pubs.acs.org.

(26) Hu, Y.; Kong, W.; Li, H.; Huang, X.; Chen, L. *Electrochem. Commun.* **2004**, *6*, 126–131.
(27) Watanabe, M.; Motoo, S. *J. Electroanal. Chem.* **1975**, *60*, 267.